

Electronic Supplementary Information

A novel cathode Li-supplement additive for high-energy and long-lifespan LIBs

Chengsifan Lei^{a,b}, Meng Huang^{*a,b}, Jinghui Chen^{a,b}, Feng Tao^{a,b}, Lei Zhang^{*a,b} and Qinyou An^{*a,b}

^aThe Sanya Science and Education Innovation Park of Wuhan University of Technology, Sanya, 572000, P. R. China.

^bState Key Laboratory of Advanced Technology for Materials Synthesis and Processing, Wuhan University of Technology, Wuhan, 430070, P. R. China.

1. Experimental

1.1 Synthesis of $\text{Li}_4\text{SiO}_4@\text{rGO}$

Lithium nitrate (LiNO_3) and silicon dioxide (SiO_2) were mixed in a 4.2:1 molar ratio and heated in a crucible at 700 °C for 4 hours to synthesize lithium metasilicate (Li_4SiO_4) powder. Subsequently, the LSO powder was uniformly dispersed in deionized water, reduced graphene oxide (rGO) was introduced at a predetermined ratio, and the mixture was milled at a speed of 350 rad min^{-1} for 4 hours to prepare the $\text{Li}_4\text{SiO}_4/\text{rGO}$ aqueous suspension. The $\text{Li}_4\text{SiO}_4/\text{rGO}$ aqueous suspension was subsequently introduced into a spray dryer at a rate of 10 mL min^{-1} at 175 °C to produce $\text{Li}_4\text{SiO}_4@\text{rGO}$ composite spheres. Additionally, this study synthesized a series of composite spheres characterized by varying mass fractions of rGO.

1.2 Preparation of electrodes

The electrode was formulated by combining the $\text{LSO}@\text{rGO}$, Super P, and polyvinylidene fluoride (PVDF) in a 7:2:1 mass ratio. These components were uniformly mixed with N-methyl-2-pyrrolidone (NMP) to create a consistent slurry. The slurry was then applied to aluminum foil with a line coater and dried at 80 °C overnight, and the mass loading of $\text{LSO}@\text{rGO}$ electrodes was 1.2 mg cm^{-2} .

The LFP and NCM622 electrodes were fabricated by blending active materials,

Super P, and PVDF in a 7:2:1 ratio using NMP, the mass loading was 3.8 mg cm⁻². For the composite electrodes, NCM622(LFP), LSO@rGO, Super P, and PVDF were mixed in a 65:5:20:10 ratio in NMP, the mass loading was 3.8 mg cm⁻². Similarly, the Gr electrode was prepared by combining active materials, Super P, and PVDF in an 8:1:1 ratio with NMP, and the mass loading was 1.2 mg cm⁻².

1.3 Materials characterizations

The material's crystal structure was analyzed via X-ray diffraction (XRD, Bruker D8 Discover, Cu K α radiation, $\lambda = 1.5418 \text{ \AA}$). Sample morphology was examined using scanning electron microscopy (SEM, JEOL JSM-7100F), while microstructure details were studied with transmission electron microscopy (TEM, JEOL JEM-F200). Fourier-transform infrared spectroscopy (FTIR, Thermo Nicolet Nexus) was employed for chemical bonding analysis. Thermal stability of LSO@rGO and LSO was assessed through thermogravimetric analysis (TGA, Q600 SDT) in air, heating from room temperature to 800 °C at 10 °C min⁻¹. Chemical composition was determined using X-ray photoelectron spectroscopy (XPS, VG Multilab 2000). For ex situ characterization, cycled electrodes were washed with diethyl carbonate (DEC) in an argon-filled glove box to eliminate impurities.

1.4 Electrochemical characterizations

CR2016 coin cells were assembled in an argon-filled glove box (H₂O and O₂ < 0.1 ppm). A 4.6 V commercial electrolyte from DodoChem and a Celgard2500 separator were used. Metallic lithium acted as the counter electrode in half-cells, while graphite served as the anode in full cells, with the N/P ratio maintained at 1.1–1.2. The electrochemical performance of half and full cells was evaluated at room temperature using the Neware system. EIS and CV measurements were performed with the EC-Lab VMP3.

2. Table

Table S1 Ionic conductivity of $\text{Li}_4\text{SiO}_4@\text{rGO}$ with different rGO contents.

rGO Content (wt%)	R (Ω)	Ionic Conductivity (S/cm) - EIS (Coin Cell System)
5%	354	1.55×10^{-4}
15%	365	1.50×10^{-4}
25%	361	1.52×10^{-4}

3. Figures

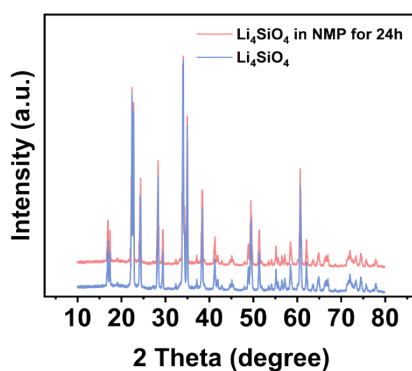


Fig. S1 XRD patterns of bare Li_4SiO_4 and Li_4SiO_4 in NMP for 24 h.

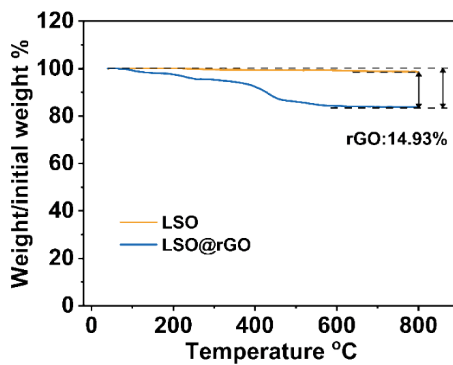


Fig. S2 TG graphs of $\text{LSO}@\text{rGO}$ and LSO.

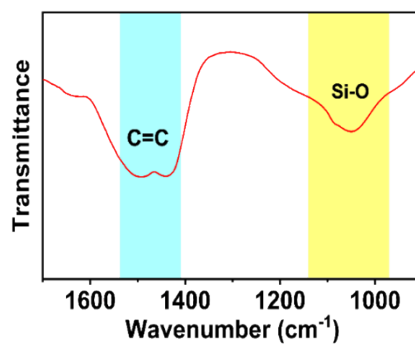


Fig. S3 FTIR spectrum of LSO@rGO.

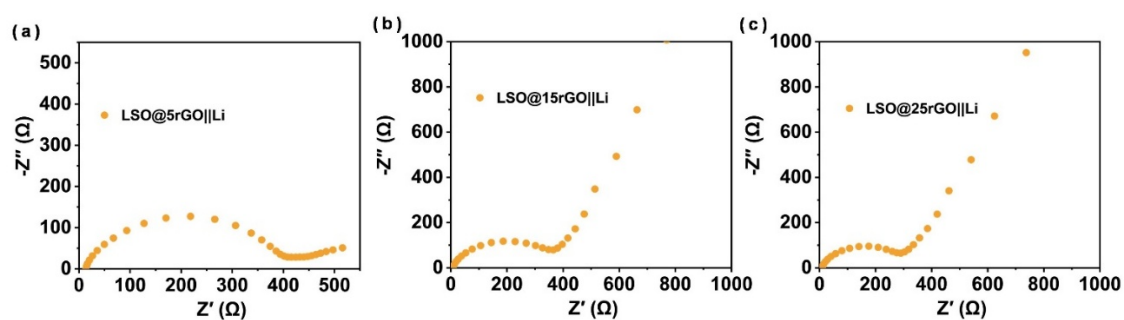


Fig. S4 EIS curves of (a) LSO@5rGO, (b) LSO@15rGO, and (c) LSO@25rGO.

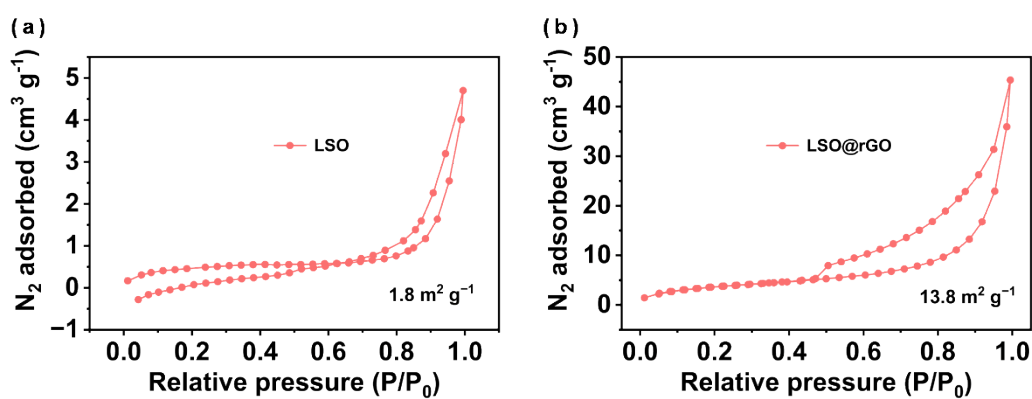


Fig. S5 N_2 adsorption-desorption isotherms of Li_4SiO_4 @rGO and Li_4SiO_4 .

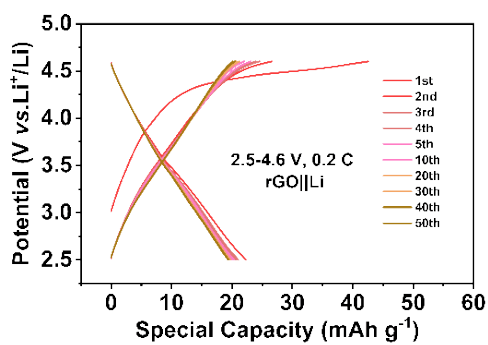


Fig. S6 The charge-discharge cycles of rGO||Li.

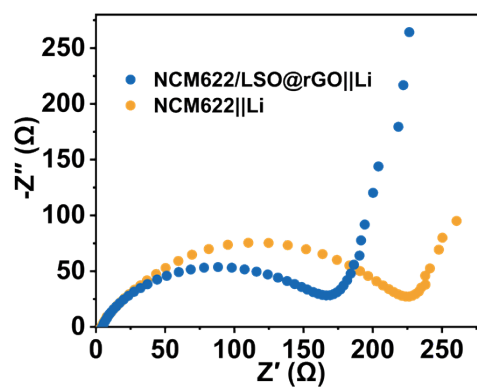


Fig. S7 EIS curves of NCM622/LSO@rGO||Li and NCM622||Li.

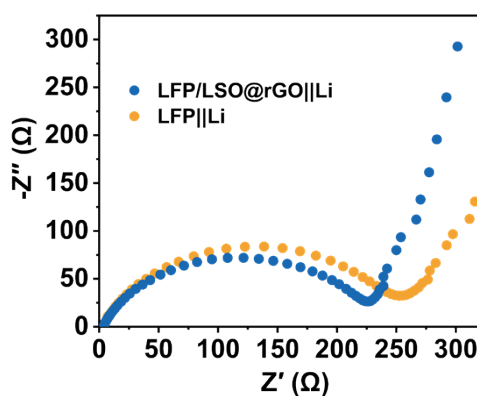


Fig. S8 EIS curves of LFP/LSO@rGO||Li and LFP ||Li.

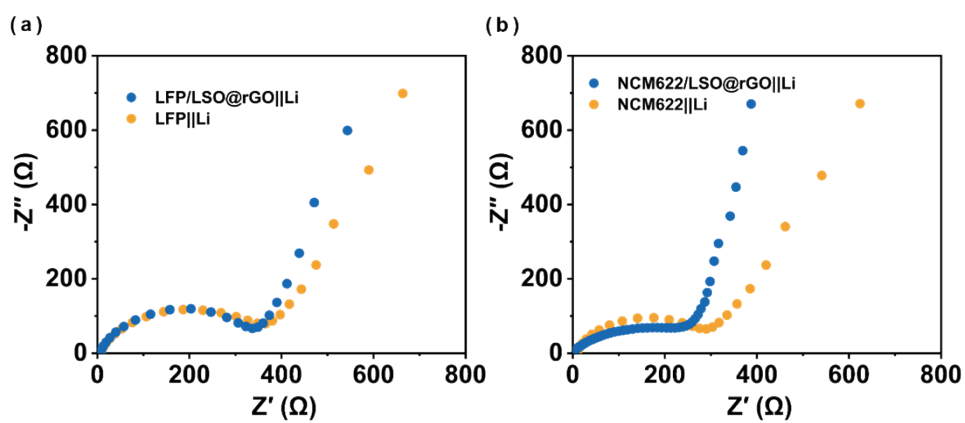


Fig. S9 EIS results after five cycles for (a) LFP/LSO@rGO||Li and LFP||Li, (b) NCM622/LSO@rGO||Li and NCM622||Li.

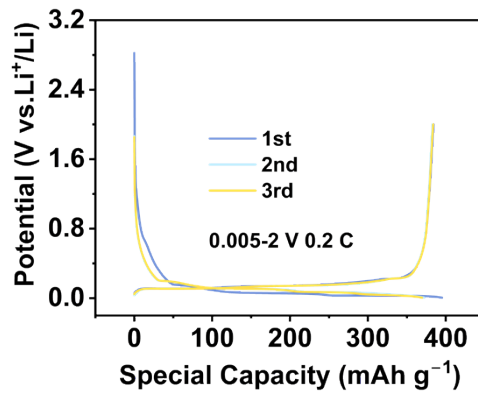


Fig. S10 The charge–discharge profiles for the initial three cycles of Gr||Li.

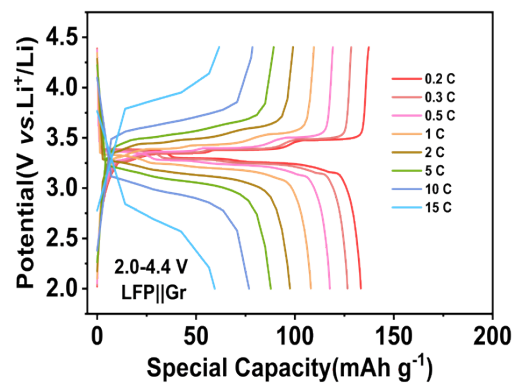


Fig. S11 Charge-discharge curves of LFP full cells at different rates. \

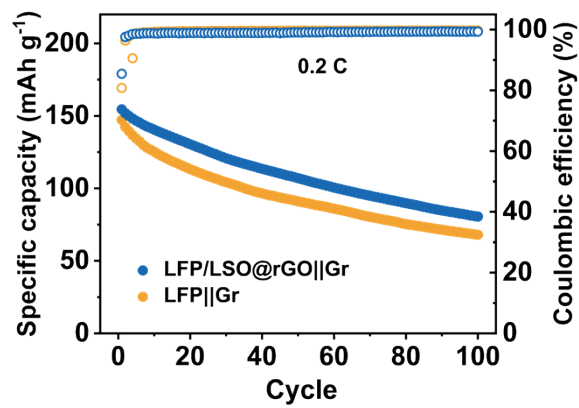


Fig. S12 Cycling performance of LFP/LSO@rGO||Gr and LFP ||Gr full cells in the range from 2.0 to 4.4 V at 0.2 C.